Ref.TH.2083-CERN

ABSORPTIVE CORRECTIONS TO THE INCLUSIVE SPECTRUM AND THE BARE TRIPLE POMERON COUPLING

A. Capella

CERN — Geneva

J. Kaplan

Laboratoire de Physique Théorique et Hautes Energies, Paris

and

J. Tran Thanh Van

Laboratoire de Physique Théorique et Particules Elémentaires, Orsay

ABSTRACT

Using the AKG cutting rules we compute the absorptive corrections to the inclusive $pp \rightarrow pX$ spectrum in the triple Regge region. The absorption corrections are very large - much larger than in the elastic amplitude - and are quite sensitive to the t dependence of the triple Pomeron coupling on its "third leg". Since this t dependence cannot be measured it is impossible to extract from inclusive data the exact value of the triple Pomeron coupling. The phenomenological consequences both for the rise with s of σ_T^{pp} and for the tests of Pomeron factorization are carefully studied.

Ref.TH.2083-CERN
28 October 1975

1. INTRODUCTION

In the perturbative approach to the Reggeon calculus, the bare triple Pomeron coupling is identified with the corresponding quantity measured in the inclusive reactions $a + b \to X + b$ near $x = 1$. As already stressed in an earlier paper[1) (hereafter referred to as I), this identification is correct, provided the absorptive corrections to the inclusive spectrum near $x = 1$ are small. If they are not, one has to take for the bare triple Pomeron coupling, a value larger than the measured quantity -- in such a way as to reproduce the inclusive data after absorption. The purpose of this work is to study the absorptive corrections mentioned above.

A general diagram contributing to the inclusive spectrum is shown in Fig. 1 (the dotted line indicates how the discontinuity is taken). However, as we stick to the perturbative approach developed in I, we neglect all graphs with more than one triple Pomeron vertex and keep only graphs of the type shown in Figs. 2 and 3. This amounts to considering absorptive corrections only between particles separated by a rapidity gap of the same order as the total rapidity interval.

The sum of all the graphs of the type shown in Fig. 2 gives the absorptive corrections to the inclusive spectrum integrated over both t (the momentum transfer between the ingoing and outgoing particle b) and M^2 (the squared mass of X). It is clear that only the particular discontinuity indicated by the dotted line in Fig. 1 contributes to the integrated inclusive spectrum. Such a discontinuity can be computed using the Abramovski, Kancheli and Gribov cutting rules[2)], suitably generalized to the graphs of Fig. 2.

Although the absorptive corrections to the integrated inclusive spectrum can be directly evaluated using the cutting rules, it is clear that in order to extract from the inclusive data the value of the triple Pomeron coupling as a function of t, one has to compute the absorptive corrections to the non-integrated inclusive spectrum, i.e. to $d\sigma/dtdM^2$. These are given by the sum of all the graphs of the type shown in Fig. 3. In order to compute these graphs, we have extended the AKG cutting rules to the non-integrated case.

Due to the combinatorial factors in the cutting rules, the size of the absorptive corrections turns out to be amazingly large. They reduce the non-absorbed contribution by a factor of 2 to 4, depending on the value of B', the t_3 slope of the triple Pomeron coupling (t_3 being the momentum transfer corresponding to its "third leg"). Since B' cannot be measured, it becomes impossible to determine from the data the exact value of the triple Pomeron coupling. The above results on the absorptive corrections, together with the analysis of the elastic data in I, allow one to determine the exact conditions under which it is possible to describe the elastic data -- and in particular the increase with s of σ_T^{pp} -- in the perturbative version of the Reggeon calculus developed in I. It turns out that with present experimental data the issue is not yet clear.

The large size of the absorptive corrections might result in a failure of Pomeron factorization. We study this point and compare the results with experimental data.

The paper is divided as follows. In Section 2 we derive the analytic expressions for the absorbed inclusive spectrum in the triple Regge region -- both integrated and non-integrated. In Section 3 we present the numerical results and discuss their implications for both the determination of the bare triple Pomeron coupling and the possibility of explaining the rise of the proton-proton total cross-section. Section 4 is devoted to tests of Pomeron factorization and Section 5 contains some concluding remarks.

2. ABSORPTIVE CORRECTIONS TO THE INCLUSIVE SPECTRUM IN THE TRIPLE REGGE REGION

First of all it has to be noticed that Figs. 2 and 3 contain blobs representing the coupling of n Pomerons to two external particles. In I we gave a recipe which allows one to compute all these blobs with a very small number of parameters. Following this recipe (depicted in Fig. 3 of I) and neglecting graphs containing the square of the triple Pomeron coupling [whose contributions are negligibly small up to ISR energies[1]], as well as graphs with quadruple Pomeron couplings, the graphs in Figs. 2 and 3 reduce respectively to the ones in Figs. 4 and 5.

We concentrate first on the integrated case (Figs. 2 and 4). According to Ref. 2, in order to compute the discontinuity in Fig. 2 one can forget about the upper and lower blobs which are not affected by the cutting[2,3]. It is therefore obvious that our model for the blob, which leads to the replacement of Fig. 2 by Fig. 4, does not affect the cutting procedure. As discussed in Ref. 2, the problem of relating the particular discontinuity in Fig. 4 to the complete imaginary part of the graph in that figure, reduces essentially to a combinatorial problem.

To illustrate the way in which we proceed, let us write down first the formula for the complete imaginary part of the graph in Fig. 4. This is given[1] by the eikonal-like expression

$$\mathrm{Im} \sum_{\ell_1+\ell_2=\ell} \left\{ \frac{-8\pi i}{\ell!} \left(\frac{i\,P(s,0)}{8\pi b_P} \right)^{\ell} \left(\frac{i\,Y(s,0)}{8\pi b_Y^a} \right) \left(\frac{1}{\frac{\ell}{b_P} + \frac{1}{b_Y^a}} \right) \times \right. \tag{1}$$

$$\left. \times \exp\left(\frac{-q^2}{\frac{\ell}{b_P} + \frac{1}{b_Y^a}} \right) \right\} X^a(\ell+1)\, X^b(\ell_1+1)\, X^b(\ell_2+1) \, .$$

Here $P(s,q^2) = P(s,0) \exp(-b_P q^2)$ and $Y^a(s,q^2) = Y^a(s,0) \exp(-b_Y^a q^2)$ are, respectively, the amplitudes for the Pomeron pole (P-graph) and Y-graph (the amplitude in Fig. 4 is the s-channel iteration of ℓ P-graphs and one Y-graph). The X's are enhancement factors due to the presence of (diffractively produced) excited states of particles a and b as intermediate states in Fig. 4 (represented by the heavy lines). We follow exactly the notations of I. The explicit forms of P, Y, and X can be found there.

Here we are not interested in the complete imaginary part of the amplitude of Fig. 4, but in the particular discontinuity shown in that figure (only that particular discontinuity contributes near $x = 1$). In order to compute it one has to distribute the ℓ Pomerons in all possible ways on both sides of the cutting line and take, according to the Cutkowsky rules, the complex conjugate of the Pomeron propagators on the right of that line. Finally, one has to sum the various terms obtained in this way:

$$\sum_{\ell_1+\ell_2=\ell} \frac{8\pi}{\ell_1!\,\ell_2!} \left(\frac{i\,P(s,0)}{8\pi\, b_P}\right)^{\ell_1} \left[\left(\frac{i\,P(s,0)}{8\pi\, b_P}\right)^{*}\right]^{\ell_2} \left(\frac{-\operatorname{Im} Y_R^a(s,0)}{8\pi\, b_{Y_R}^a}\right) \times$$
$$\times \left(\frac{1}{\frac{\ell_1}{b_P} + \frac{\ell_2}{b_P^*} + \frac{1}{b_{Y_R}^a}}\right) X^a(\ell+1)\, X^b(\ell_1+1)\, X^b(\ell_2+1) \quad . \tag{2}$$

This differs from expression (1) for the total imaginary part, in the following respects:

i) One takes the complex conjugate of the ℓ_2 Pomerons on the right of the cutting line.

ii) Y^a and b_Y^a are replaced by $-\operatorname{Im} Y_R^a$ and $b_{Y_R}^a$, respectively, where Y_R^a ($b_{Y_R}^a$) is identical to Y^a (b_Y^a), except for the fact that the phases coming from the signature factors have been suppressed. This is, of course, due to the fact that cutting the Y-graph, in the way depicted in Fig. 4, amounts to taking the imaginary part of the expression for the Y-graph in which the product $\xi_1\xi_2$ of the signature factors of the Pomerons 1 and 2 has been replaced by[†)] $\xi_1\xi_2^*$.

iii) The factor $1/\ell!$ in expression (1) is replaced by $1/(\ell_1!\,\ell_2!)$.

---

†) Strictly speaking the phases in the Y-graph only disappear completely when the four-momenta of Pomerons 1 and 2 are equal. We have taken $\xi_1(q_1^2)\, \xi_2^*(q_2^2) \equiv 1$. This is a good approximation on account of the peaking of all vertices at $q^2 = 0$. Without this approximation it is not possible to integrate analytically the inclusive $d\sigma/dt dM^2$.

The derivation of expression (2) and its equivalence to the AKG cutting rules is discussed in detail in the Appendix. Notice that, in the case of a purely imaginary Pomeron propagator, the ratio of expression (2) to expression (1) is equal to

$$-\sum_{\ell_1+\ell_2=\ell} \frac{\ell!}{\ell_1!\,\ell_2!} = -2^{\ell} . \tag{3}$$

This makes the absorptive series for the inclusive spectrum different from the corresponding series for the elastic amplitude and is responsible for the larger size of the absorptive corrections in the former.

It is now easy to extend formula (2) to the non-integrated case (Fig. 5). Indeed, all one has to do is to replace $-\mathrm{Im}\, Y^a_R$ in (2) by the triple Pomeron expression for $d\sigma/dtdM^2$ (normalized in such a way that integrating it over M^2 and t one gets back $-\mathrm{Im}\, Y^a_R$). Taking exponential forms for the particle-particle-Pomeron coupling and for the triple Pomeron coupling

$$\begin{aligned} g_{aaP}(q^2) &= g_a \exp(-q^2 A_a/2) \\ r(k_1^2, k_2^2, (\vec{k}_1-\vec{k}_2)^2) &= r \exp\{-B(k_1^2+k_2^2)/2 - B'(\vec{k}_1-\vec{k}_2)^2/2\}, \end{aligned} \tag{4}$$

one can write the following expression for the discontinuity in Fig. 5:

$$\sum_{\ell_1+\ell_2=\ell} \frac{g_a g_b^2 r}{16\pi s^2} \iint \frac{d\vec{k}_1}{8\pi^2}\frac{d\vec{k}_2}{8\pi^2} \left(\frac{s}{M^2}\right)^{\alpha(k_1^2)+\alpha(k_2)^2} (M^2)^{\alpha[(\vec{k}_1-\vec{k}_2)^2]} \times$$

$$\times \exp\left\{-i\frac{\pi}{2}\alpha'(k_1^2-k_2^2)\right\} \exp\{-(A_a+B)(k_1^2+k_2^2)/2-(A_a+B')(\vec{k}_1-\vec{k}_2)^2/2\}$$

$$\times A_{\ell_1}[s,(\vec{q}-\vec{k}_1)^2]\, A^*_{\ell_2}[s,(\vec{q}-\vec{k}_2)^2]\, X^a(\ell+1)\, X^b(\ell_1+1)\, X^b(\ell_2+1) ,$$

where $\vec{k}_1$ and $\vec{k}_2$ are two-dimensional vectors (see Fig. 5), $t \sim (-\vec{q})^2$ is the momentum transfer between the incoming and outgoing particle b, and A_{ℓ_i} is the amplitude for the s-channel iteration of ℓ_i Pomerons given by the eikonal formula

$$A_{\ell_i}(s,q^2) = -\frac{8\pi i}{\ell_i!}\left(\frac{i\,P(s,0)}{8\pi b_P}\right)^{\ell_i} \frac{b_P}{\ell_i} \exp\left(-\frac{b_P}{\ell_i} q^2\right).$$

Performing the integration in $\vec{k}_1$ and $\vec{k}_2$ one gets

$$\sum_{\ell_1+\ell_2=\ell} \frac{g_a g_b^2 r}{16\pi s^2}\, s^{1+\Delta} \left(\frac{s}{M^2}\right)^{1+\Delta} \frac{b_P b_P^*}{D_{\ell_1 \ell_2}} \left(\frac{i P(1,0)}{8\pi b_P}\right)^{\ell_1} \times \tag{5}$$

$$\times \left[\left(\frac{i P(1,0)}{8\pi b_P}\right)^*\right]^{\ell_2} \exp\{-E_{\ell_1 \ell_2} q^2\} \exp\{-(\alpha+\alpha^*) q^2_{min}\} X^a(\ell+1) X^b(\ell_1+1) X^b(\ell_2+1),$$

where $1 + \Delta$ is the intercept of the Pomeron, q^2_{min} is the minimum value of the momentum transfer, and

$$\alpha = \frac{A+B}{2} + \alpha'\left(\ln \frac{s}{M^2} - i\frac{\pi}{2}\right),$$

$$\beta = \frac{A+B'}{2} + \alpha' \ln M^2,$$

$$D_{\ell_1 \ell_2} = \left(b_P + \ell_1(\alpha_1+\beta)\right)\left(b_P^* + \ell_2(\alpha_2+\beta)\right) - \ell_1 \ell_2 \beta^2,$$

$$E_{\ell_1 \ell_2} = \left\{(\alpha+\alpha^*) b_P b_P^* + (\ell_1 b_P^* + \ell_2 b_P)\left[\alpha\alpha^* + \beta(\alpha+\alpha^*)\right]\right\} \times [D_{\ell_1 \ell_2}]^{-1}$$

Formula (5) gives the expression for the absorbed inclusive $d\sigma/dq^2dM^2$ obtained by a natural extension of the AKG cutting rules.

As a matter of fact, integrating expression (5) over M^2 and t one would get back expression (2), although only approximately because of the approximation needed to obtain (2). Although (5) cannot be integrated analytically one can check it numerically by comparing Tables 1 and 2 in the next section.

3. ABSORPTIVE CORRECTIONS, DETERMINATION OF THE BARE TRIPLE POMERON COUPLING AND RISE OF σ_T.

In this section we compute numerically the absorptive corrections which result from formulae (2) and (5), using some realistic values of the parameters. We shall restrict ourselves to $pp \to pX$ inclusive reactions. In I we found that a very good description of all existing elastic data near $t = 0$ can be obtained, in perturbative Reggeon calculus, with the following values of the parameters:

$$\alpha(0) = 1+\Delta \quad (\Delta = 0.1275), \quad C = g_P^3 r / 16\pi\alpha' = 1\ mb (GeV)^{-2}, \tag{6}$$

$$g_P^2 = 22.75\ mb, \quad \alpha' = 0.25\ (GeV)^{-2}, \quad A_P = 3.3\ (GeV)^{-2}, \quad B = B' = 1\ (GeV)^{-2}.$$

The value of B' is not directly measurable and therefore it is important to study changes in the absorptive corrections due to changes in this parameter.

The values of the integrated $pp \to pX$ inclusive spectrum before and after absorption for different values of s and B' are given in Table 1.

The absorptive corrections to the non-integrated $d\sigma/dtdM^2$ [formula (5)] for different values of s, t, M^2 and B' are given in Table 2.

It can be seen from Tables 1 and 2 that both the M^2-dependence and the t-dependence of $d\sigma/dtdM^2$ are little affected by the absorptive corrections, especially for $B' \geq 1$ *). Likewise, the absorptive corrections affect very little the s-dependence of the inclusive spectrum**). However, the size of the absorptive corrections is amazingly large and very sensitive to the value of B'. As a consequence, the value of $d\sigma/dtdM^2$ (for small $|t|$ and $x \sim 1$), as well as its integral over M^2 and t, is reduced by a factor of two to four depending on the value of B'. Therefore, in order to reproduce the inclusive data one has to take a value of the triple Pomeron coupling larger than the corresponding value measured experimentally (in such a way that the experimental value is obtained after absorption). Since the value of B' is unknown, it becomes impossible to extract from the data the exact value of the triple Pomeron coupling -- no matter how precise the available data are. One could object that the experimentally measured triple Pomeron coupling is an effective coupling (which includes the absorptive correction) and that one can use this effective coupling in computing, for instance, the elastic amplitude. Of course, to be consistent, one should not include absorptive corrections in computing the latter, since the effective coupling takes care of them. Unfortunately this argument is not correct. Indeed, the absorptive corrections to the inclusive spectrum in the triple Regge region are much larger than the ones in the elastic amplitude and, furthermore, their relative strength in the two cases depends on the value of B'. All this can be seen from Eqs. (1) and (2) and is a mathematical result that follows from the AKG cutting rules.

Let us turn now to the rise with s of σ_T^{pp}. It was shown in I that when the value of the triple Pomeron coupling is too large it is not possible, in

---

*) Their main effect is to give some concavity to the t-dependence, which seems to be consistent with data[4]. The absorbed spectrum has, of course, a steeper t-dependence at small $|t|$, but there is a cross-over at $|t| \sim 1$ GeV^2.

**) In particular, absorbtive effects, although going in the right direction, will not alter the fact that the PPP contribution increases with s for $\alpha_P(0) \sim 1.13$. This appears to be in contradiction with recent FNAL data[5]. However, we have checked that a small RRR contribution together with the usual RRP one, are sufficient to heal this disease thanks to their s^{-1} energy dependence.

perturbative Reggeon calculus, to reproduce the observed rise of σ_T^{pp} no matter how large the bare Pomeron intercept is. As discussed above, the amount of absorption, and consequently the value of the triple Pomeron coupling, increases for decreasing values of B′. Therefore, the bound on the strength of the triple Pomeron coupling (required in order to reproduce the rise of σ_T^{pp}) will result in a bound on the value of B′. In the following we consider this point in some detail. First we discuss the experimental situation. The FNAL data[5] on pp → pX, for incident proton momentum from 150 to 400 GeV/c, in the region $0.03 < |t| < 0.12$ and $x \leq 0.95$, can be fitted by[5,6]

$$\frac{d\sigma}{dt\, dM^2} = \frac{A(1 + B/p_{lab})}{M^2} \exp(bt) \,, \tag{7}$$

with $A = 3.5 \pm 0.4$ mb, $B = 54 \pm 16$ GeV and $b = 6.5 \pm 0.3\ (\mathrm{GeV})^{-2}$. Two independent triple Regge fits to all pp → pX data [presented by Olsen and Sannes at the last Moriond meeting[7]] give, for the PPP contribution to Eq. (7), $A_{PPP} = 2.0$ mb and $A_{PPP} = 2.1$ mb, respectively. However, a more recent fit due to Desai et al.[8] gives $A_{PPP} = 2.9$ mb. Although this last value seems rather high, we shall examine the two extreme cases $A_{PPP} = 2$ mb (which was the value used in I) and $A_{PPP} = 2.9$ mb. The resulting bound on B′ is qualitatively different in the two cases. With $A_{PPP} = 2$ mb one gets $B' \geq 0$ which is quite reasonable, whereas for $A_{PPP} = 2.9$ mb one gets $B' \gtrsim 40\ (\mathrm{GeV})^{-2}$ which is physically untenable.

Let us discuss the effective computation of the above bounds on B′. These can be obtained from the results given in Table 3. In this table we give, for several values of B′, the experimental value A_{PPP}^{exp} (for which we consider the two values discussed above), the theoretical value A_{PPP}^{th}, i.e. the value of A_{PPP} that gives A_{PPP}^{exp} after absorption (obtained by multiplying A_{PPP}^{exp} by the absorptive ratio in Table 1), and A_{PPP}^{max}, i.e. the maximum value of A_{PPP}^{th} allowing a fit to the elastic proton-proton data*). The value of A_{PPP}^{max} for $B' = 1$ follows from the analysis in I. More precisely, in I we obtained for $B' = 1$, the maximum value (allowing one to reproduce the elastic data) of a quantity C defined as $C = A_{PPP}^{th}\ (s/M^2)^{2[1-\alpha_P(0)]} (M^2)^{1-\alpha_P(0)}$. This gives $C \sim A_{PPP/4}^{th}$ for $s = 700\ \mathrm{GeV}^2$ and M^2 in the diffractive peak ($M^2 \simeq 10$-$20\ \mathrm{GeV}^2$). The value of A_{PPP}^{max} (or C^{max}) decreases when B′ increases, because the contribution of the Y-graph to σ_T is less and less absorbed when B′ increases. The ratio R of the values of that contribution before and after absorption [obtained from Eq. (1)] is given in the last column of Table 3. The value of A_{PPP}^{max} for $B' \neq 1$ is, obviously, given by $A_{PPP}^{max}(B') = [R(B')/R(B'{=}1)]\ A_{PPP}^{max}(B'{=}1)$.

*) Most of the quantities in Table 1 depend slightly on the value of s. For definiteness we take $s = 700\ \mathrm{GeV}^2$.

We see from Table 3 that, for $A^{exp}_{PPP} = 2$ mb, the value $B' = -3$ is excluded, because it requires A^{th}_{PPP} larger than A^{max}_{PPP}, whereas the other values of B' in the table are acceptable. On the contrary, for $A^{exp}_{PPP} = 2.9$ mb all values of B' smaller than or equal to 40 are excluded.

In conclusion, if future data confirm the value $A^{exp}_{PPP} \sim 2$ mb, the analysis of the elastic data in I remains valid and gives the interesting bound $B' \gtrsim 0$ on this otherwise unknown quantity. However, if $A^{exp}_{PPP} \sim 3$ mb turns out to be correct, then it is not possible to reproduce the elastic data -- and in particular the energy dependence of σ^{pp}_T -- no matter how large one takes the bare Pomeron intercept.

4. TEST OF THE POMERON FACTORIZATION

One of the characteristics of Gribov Reggeon calculus is the presence of large contributions of *a priori* non-factorizable graphs. This is due to the fact that the two most important graphs besides the pole, i.e. the two-Pomeron cut and the Y-graph are both negative. This is different from the situation in models[9] where the corrections to the pole contribution are small -- due for instance to the fact that the Y-graph is taken with a positive sign and cancels in part the two-Pomeron cut.

A striking manifestation of the above characteristic is the large size of the absorptive corrections to the inclusive spectrum computed in the preceding section. These corrections might produce a large breaking of Pomeron factorization, which is known to be very well satisfied in inclusive reactions. Indeed, if the Pomeron factorizes, the ratio of the $p\pi^- \to pX$ over the $pp \to pX$ inclusive cross-sections in the triple Regge region should be equal to the ratio $\sigma^{\pi^-p}_T/\sigma^{pp}_T$. This has been accurately shown to be the case[10]. It can be seen in Fig. 6 that surprisingly enough, this result is maintained when the absorptive corrections are taken into account.

A more direct test of the Pomeron factorization results from the analysis in I. It turns out that the ratio $\sigma^{pp}_T/\sigma^{\pi p}_T$ is equal to the corresponding ratio of the bare Pomeron pole terms.

The latter result, together with the well-known result that the AKG cutting rules lead to a cancellation of the absorptive corrections to the inclusive spectra in the central region, leads to

$$\frac{1}{\sigma^{ab}_T} \left.\frac{d\sigma}{dy}\right|_{ab\to cX} = \frac{1}{\sigma^{a'b}_T} \left.\frac{d\sigma}{dy}\right|_{a'b\to cX} ,$$

in the central region.

We do not think that the above results are a mere coincidence. On the contrary their origin can be traced[11] to the fact that the absorptive corrections to, say, the inclusive spectrum in the triple Regge region depend roughly on the ratio of σ_T to the forward elastic slope (for instance the size of the absorptive corrections in Fig. 4 is larger for larger σ_T^{ab} and smaller for a larger t-slope of the elastic ab differential cross-section). Since the above ratio is roughly the same for πp and pp scattering one expects that the relative amount of absorption will be roughly the same in both reactions, leaving the ratio of inclusive, as well as total, cross-sections practically unchanged.

In any case, the above results show that a test of factorization is by no means a test of the dominance of the scattering processes by a simple pole. Therefore the relevant tests of Pomeron factorization will be those in which total and production cross-sections are simultaneously involved. For instance the factorization relation

$$\frac{d\sigma}{dt_1\, dt_2\, dM^2} = \frac{d\sigma}{dt_1\, dM^2}\, \frac{d\sigma}{dt_2\, dM^2} \Big/ \sigma_T \,, \tag{8}$$

where the left-hand side represents double Pomeron cross-section, holds for large M^2 ($M^2 \gtrsim 5$ GeV^2) if one neglects absorptive corrections. However, we have seen that the absorptive corrections in $d\sigma/dtdM^2$ and in σ_T are rather different and therefore one expects (8) to break down. (The same is true in the case of double diffraction). Using the set of parameters (6) we find that the left-hand side in (8) may be larger than the right-hand side by a factor of 1.5 to 2. This can provide an interesting test of the AKG cutting rules.

5. CONCLUSIONS

This paper is complementary to the ones in Ref. 1. In this series of papers we have developed a simple version of the perturbative Reggeon calculus. The main assumptions are: (a) the fact of neglecting quadruple Pomeron couplings (and higher) and (b) the use of a simple model for the two particles - n Pomerons blob (which allows one to express them in terms of experimentally known low-energy quantities and the triple Pomeron coupling). When the bare Pomeron intercept is chosen to correspond to a renormalized Pomeron intercept exactly equal to one (critical Pomeron), we find no increase whatsoever of the total proton-proton cross-section in the whole ISR energy range. This result was obtained in the second paper of Ref. 1 and, although absorptive corrections were ignored, it remains true when they are taken into account. There are two reasons for this:

i) As discussed above the absorptive corrections force one to take a bare triple Pomeron coupling larger than the measured quantity. On the other hand, the fact that the bare Pomeron intercept is above one $[\alpha(0) = 1 + \Delta]$ forces one to take a bare triple Pomeron coupling smaller than that corresponding to $\alpha(0) = 1$ by a factor $(s/M^2)^{2\Delta}(M^2)^{\Delta}$. These two facts, which were both ignored in the aforementioned paper[1] tend to cancel each other (see Section 3).

ii) The exact formulation of the above result is as follows: the increase $(\Delta\sigma_T)^{pp}$ with s of σ_T^{pp} in the ISR energy range depends essentially on two parameters, the bare Pomeron coupling A_{PPP} and the bare Pomeron intercept. When these two parameters are related in such a way that the Pomeron is critical, then $(\Delta\sigma_T)^{pp}$ is essentially zero, not only when A_{PPP} is taken equal to its measured value but for a large range of values of this parameter. Therefore the result is independent of changes in A_{PPP} resulting from absorptive corrections. It is also independent of the exact value of B' [defined in Eq. (4)]. Furthermore, we believe that this result, due to its generality, is not much affected by the detailed assumptions in our model (such as neglecting quadruple Pomeron coupling, etc.).

In the first paper of Ref. 1 we presented a detailed phenomenological study of the perturbative Reggeon calculus and showed that when Δ is taken to be a positive free parameter, roughly ten times larger than its critical value, one can describe beautifully all elastic data (at least near $t = 0$) and total cross-sections from 10 GeV up to the highest ISR energies with very few parameters. This detailed analysis is of course sensitive to the absorptive corrections. These corrections were taken into account in that paper in a phenomenological way by presenting fits for different values of A_{PPP} -- in particular for values of A_{PPP} two and even three times larger than its measured value. The result is that acceptable fits exist only when A_{PPP} is not too large. This is due to the fact that $(\Delta\sigma_T)^{pp}$ in the ISR energy range cannot be made bigger and bigger with increasing values of Δ. On the contrary, it reaches a maximum and then decreases. The value of $(\Delta\sigma_T)^{pp}$ at the maximum depends on the value of the triple Pomeron coupling and decreases when the triple Pomeron coupling increases. Therefore fits only exist for A_{PPP} not larger than some A_{PPP}^{max}.

In order to obtain the value of the triple Pomeron coupling from the inclusive data, one has to compute the inclusive cross-section with the same version of the perturbative Reggeon calculus as used in elastic scattering. In particular, some absorptive corrections must be taken into account. This requires the AKG cutting rules. It is a consequence of these rules that the absorptive series for the inclusive processes in the triple Regge region is different from the corresponding series for the contribution of those processes to the total cross-section. The terms of the former series are enhanced by combinatorial factors. As a result, the absorptive corrections are much larger in the inclusive spectrum near $x = 1$

than in the total cross-section. They have the effect of reducing the non-absorbed values of $d\sigma/dtdM^2$ by a factor of 3 or even 4. Thus, in order to get the value of the bare triple Pomeron coupling, one has to multiply by that factor the measured quantity.

It turns out, however, that the absorptive corrections are very sensitive to the t-slope (B') of the triple Pomeron coupling or its "third leg". Since this quantity cannot be measured, it becomes impossible to determine the exact value of the bare triple Pomeron coupling (even if the renormalization effects due to loops are small at present energies the absorptive effects are important and depend on an unknown quantity).

What it is possible to do, however, is to use the measured value of the triple Pomeron coupling, together with the result (mentioned above) that the bare triple Pomeron coupling cannot be larger than some A_{PPP}^{max} -- in order to get a bound on the value of B'. Using the smallest experimental value of the triple Pomeron coupling (A_{PPP} = 2 mb) one gets the very satisfactory bound $B' \gtrsim 0$. However, using the largest one (A_{PPP} = 2.9 mb) one gets the bound $B' \gtrsim 40$ $(GeV)^{-2}$, which is, of course, totally unacceptable. This does not mean that the results in the first paper in Ref. 1 are very sensitive to the exact value of B'. On the contrary, it means that since A_{PPP} = 2.9 mb is larger than A_{PPP}^{max} (= 2 mb) for B' = 1 and since the results in that reference depend very little on B', one gets unreasonable values of this quantity when one tries to save the situation by changing B'. However, the fact that A_{PPP} = 2.9 mb seems to be consistent with the data available at present makes it impossible to come to a definite conclusion on the issue of the perturbative Reggeon calculus, at least with its simple version used here.

Of course, the above figures are only true in our version of the perturbative Reggeon calculus and may change when using a more sophisticated model for the two particles - n Pomerons blob and/or by including a quadruple Pomeron coupling, etc. However, our results should remain qualitatively true. We hope that more precise data will lead to a value of the triple Pomeron coupling close to A_{PPP} = 2 mb $(GeV)^{-2}$. In this case a simple perturbative Reggeon calculus will remain as an attractive possibility and will deserve further investigation.

Finally, an interesting result concerning Pomeron factorization in the perturbative Reggeon calculus is given in Section 4. We show that some tests of Pomeron factorization remain true, at a 5-10% level, despite the presence of very large absorptive corrections and we suggest significant tests which are expected to fail in the presence of those corrections.

Acknowledgements

It is a pleasure to thank L. Caneschi, A. Schwimmer, G. Thomas, and especially A. Kaidalov and M. Le Bellac, for useful discussions.

APPENDIX

In order to derive Eq. (2) we show here how the combinatorial factors of the AKG cutting rules can be extended to the case of a Reggeon diagram consisting of $\nu - 1$ P-graphs and one Y-graph.

For clarity, let us repeat first the case of a diagram with ν P-graphs[2]. The complete discontinuity, D, of such a graph can be symbolically written as follows [cf. Eq. (1)]:

$$D = 2\,\mathrm{Im}\left\{-\frac{i}{\nu!}\,[iP]^{\nu}\right\} = -\frac{2}{\nu!}\,\mathrm{Re}\,[iP]^{\nu}. \tag{A.1}$$

Consider now the discontinuities F^{ν}_{μ} obtained by cutting μ out of the ν Pomeron. According to (A.1), taking the discontinuity through one Pomeron propagator amounts to replacing iP by

$$-2\,\mathrm{Re}\,(iP) = 2\,\mathrm{Im}\,P = -\,[iP + (iP)^{*}]. \tag{A.2}$$

Furthermore, each Pomeron can be situated either to the right or to the left of the cutting line. For the former one has to replace (iP) by $(iP)^{*}$. Choosing the μ-cut Pomerons in all possible ways one finally gets

$$\begin{aligned} F^{\nu}_{\mu\neq 0} &= \frac{\binom{\nu}{\mu}}{\nu!}\,(-)^{\mu}\,[iP+(iP)^{*}]^{\mu}\,[iP+(iP)^{*}]^{\nu-\mu} = \\ &= \frac{(-)^{\mu}}{(\nu-\mu)!\,\mu!}\,[iP+(iP)^{*}]^{\nu}. \end{aligned} \tag{A.3}$$

When slicing the ν-Pomerons diagram, in between Pomerons one gets an expression analogous to (A.3) except for the absence of the factor $(-)^{\mu}\binom{\nu}{\mu}$, i.e.

$$F^{\nu}_{0} = \frac{1}{\nu!}\,[iP+(iP)^{*}]^{\nu} - \frac{1}{\nu!}\,[iP]^{\nu} - \frac{1}{\nu!}\,[(iP)^{*}]^{\nu}, \tag{A.4}$$

where we have subtracted the last two terms which do not correspond to a cut in between Pomerons, since all of them are on the same side of the cutting line. Using $\Sigma^{\nu}_{\mu=1}\binom{\nu}{\mu}(-)^{\mu} = -1$, one gets immediately the saturation condition

$$F^{\nu}_{0} + \sum_{\mu=1}^{\nu} F^{\nu}_{\mu} = \frac{1}{\nu!}\left\{[iP]^{\nu} + [(iP)^{*}]^{\nu}\right\} = D. \tag{A.5}$$

We turn now to the case of a Reggeon diagram consisting of $\nu - 1$ P-graph and one Y-graph. The total discontinuity of the amplitude is then given by

$$D = 2\,\mathrm{Im}\left\{\frac{-i}{(\nu-1)!}\,[iP]^{\nu-1}[iY]\right\}, \tag{A.6}$$

quite analogous to (A.1). However, the expression for $F^{\nu}_{\mu\neq 1}$ will be now the sum of two terms corresponding to whether or not the Y-graph is cut:

$$\begin{aligned} F^{\nu}_{\mu\,(0<\mu<\nu)} = {} & \frac{1}{(\nu-1)!}\binom{\nu-1}{\mu}(-)^{\mu}\left[iP+(iP)^*\right]^{\mu}\times \\ & \times\left[iP+(iP)^*\right]^{\nu-\mu-1}\left[iY+(iY)^*\right]+ \\ & +\frac{1}{(\nu-1)!}\binom{\nu-1}{\mu-1}(-)^{\mu-1}\left[iP+(iP)^*\right]^{\mu-1}\times \\ & \times\left[iP+(iP)^*\right]^{\nu-\mu}\left[\mathrm{Dis}\,(iY)\right], \end{aligned} \tag{A.7}$$

where Dis (iY) means the complete discontinuity of the Y-graph, which can itself be sliced in different ways. For $\mu = \nu$ the first term in (A.7) is, of course, not present and one has

$$F^{\nu}_{\nu} = \frac{1}{(\nu-1)!}(-)^{\nu-1}\left[iP+(iP)^*\right]^{\nu-1}\left[\mathrm{Dis}\,(iY)\right] \tag{A.8}$$

Finally,

$$\begin{aligned} F^{\nu}_{0} = {} & \frac{1}{(\nu-1)!}\left[iP+(iP)^*\right]^{\nu-1}\left[iY+(iY)^*\right]- \\ & -\frac{1}{(\nu-1)!}[iP]^{\nu-1}[iY]-\frac{1}{(\nu-1)!}\left[(iP)^*\right]^{\nu-1}\left[(iY)^*\right]. \end{aligned} \tag{A.9}$$

The saturation of the complete discontinuity [Eq. (A.1)] also holds here. This is true independently of the form of the complete discontinuity of the Y-graph. Indeed, the sum of all the terms proportional to Dis (iY) cancels. This can be seen from the relation

$$\begin{aligned} \sum_{\mu=1}^{\nu-1}\binom{\nu-1}{\mu-1}(-)^{\mu-1}+(-)^{\nu-1} & = \sum_{\mu=1}^{\nu}\binom{\nu-1}{\mu-1}(-)^{\mu-1} = \\ & = \sum_{\lambda=0}^{\nu-1}\binom{\nu-1}{\lambda}(-)^{\lambda} = 0. \end{aligned} \tag{A.10}$$

The argument above is, of course, valid when the Y-graph is replaced by an arbitrary graph. Due to the cancellation (A.10), the saturation property (A.1) can be proved without specifying the various discontinuities of the Y-graph (or of any arbitrarily complicated graph by which the latter can be replaced).

The cancellation (A.10) is analogous to the one in Ref (2) for the case of the absorptive corrections to the inclusive spectrum in the central region. However, when one considers the inclusive spectrum near x = 1, the above cancellation does not hold, because the discontinuities obtained by cutting simultaneously the Y-graph and one or more Pomerons do not contribute to that phase-space region. Only the discontinuity in Fig. 4 does contribute near x = 1. This discontinuity is given by the second term of Eq. (A.7) with $\mu = 1$, i.e.

$$\frac{1}{(\nu-1)!}\left[i\mathcal{P} + (i\mathcal{P})^{*}\right]^{\nu-1}\left[\mathrm{Dis}\,(iY)\right],$$

where one has to replace Dis (iY) by the particular discontinuity of the Y-graph shown in Fig. 4. With the definition of Y^R given in the main text (and with the approximation for the phases described there) this discontinuity is precisely equal to $-2\,\mathrm{Im}\,Y_R\,(s,0)$. We get, in this way, Eq. (2) of the main text.

REFERENCES

1) A. Capella, J. Tran Thanh Van and J. Kaplan, Nuclear Phys. B27, 493 (1975).
A. Capella and J. Kaplan, Phys. Letters 52B, 448 (1974).

2) V.A. Abramovski, O.V. Kancheli and V.N. Gribov, *in* Proc. 16th Internat. Conf. on High-Energy Physics, Chicago-Batavia, 1972 (National Accelerator Laboratory, Batavia, 1972).

3) M. Baker and L.D. McLerran, University of Washington preprint, The physical basis of the Reggeon Calculus and its s-channel structure, and to be published in Proc. EPS Internat. Conf. on High-Energy Physics, Palermo, 1975.
M. Ciafaloni, G. Marchesini and G. Veneziano, A topological expansion for high-energy hadron collisions, to be published in Nuclear Phys.
J. Koplik and A.H. Mueller, Columbia preprint.

4) M.G. Albrow et al., Nuclear Phys. B72, 376 (1974).

5) Y. Akimov et al., Fermilab Pub-75/26-EXP.

6) K. Goulianos, Rockefeller University preprint (1974).

7) S. Olsen, *in* Proc. 10th Rencontre de Moriond, 1975 (ed. J. Tran Thanh Van) (Lab. de Phys. Theor. et Part. Elem., Orsay, 1975).
F. Sannes, *in* Proc. 10th Rencontre de Moriond, 1975 (ed. J. Tran Thanh Van) (Lab. de Phys. Theor. et Part. Elem., Orsay, 1975).

8) B.R. Desai (private communication).

9) M. Bishari, Phys. Letters 56B, 355 (1975).
P.V.V. Collins, F.D. Gault and A. Martin, Phys. Letters 47B, 239 (1973) and to be published in Nuclear Phys.

10) F.C. Winkelman, preprint LBL 2459 (1973).

11) A.B. Kaidalov, Soviet J. Nuclear Phys. 16, 217 (1973).

Table 1

The integrated values of $d\sigma/dM^2dt$ before and after absorption, computed from Eq. (2), for different values of the parameter B' [defined in Eq. (4)] and two different values of s. The upper five values correspond to s = 700 GeV^2 and the lower five to s = 2800 GeV^2.

B' [$(GeV)^{-2}$]	Non-abs. [mb]	Abs. [mb]	Abs./Non-abs.
- 3	2.34	0.55	4.25
+ 1	2.34	0.81	2.89
+ 5	2.34	1.01	2.32
+10	2.34	1.21	1.93
+40	2.34	1.76	1.33
- 3	3.89	0.84	4.63
+ 1	3.89	1.23	3.16
+ 5	3.89	1.55	2.51
+10	3.89	1.88	2.07
+40	3.89	2.81	1.38

Table 2

The values of $d\sigma/dtdM^2$ before and after absorption, as computed from Eq. (5), are given for two different values of M^2 and t. The figures in this table correspond to s = 700 GeV^2 and $B' = 1\ (GeV)^{-2}$.

M^2 [GeV^2]	$-t$ [GeV^2]	$(d\sigma/dtdM^2)_{non-abs}$ [$mb\,(GeV)^{-4}$]	$(d\sigma/dtdM^2)_{abs}$ [$mb\,(GeV)^{-4}$]	Ratio
10	0.05	0.288	0.102	2.81
30	0.05	0.0856	0.0309	2.77
10	0.25	0.0796	0.0247	3.23
30	0.25	0.264	0.00858	3.08

Table 3

The values of A^{th}_{PPP}, A^{max}_{PPP} and R, defined in the main text, are given for different values of B′ and two extreme values of the measured triple Pomeron coupling A^{exp}_{PPP} [as defined in (7)]. The values of B′ for which A^{th}_{PPP} is larger than A^{max}_{PPP} are not acceptable, because they correspond to situations in which it is not possible to describe the elastic data and the energy behaviour of σ^{pp}_{T}.

B′ [GeV^{-2}]	A^{exp}_{PPP} [mb]	A^{th}_{PPP} [mb]	A^{max}_{PPP} [mb]	R
− 3	2.0 (2.9)	8.50 (12.32)	7.42	2.30
+ 1	2.0 (2.9)	5.78 (8.38)	6.00	1.86
+ 5	2.0 (2.9)	4.64 (6.73)	5.32	1.65
+10	2.0 (2.9)	3.86 (5.60)	4.81	1.49
+40	2.0 (2.9)	2.66 (3.86)	3.84	1.19

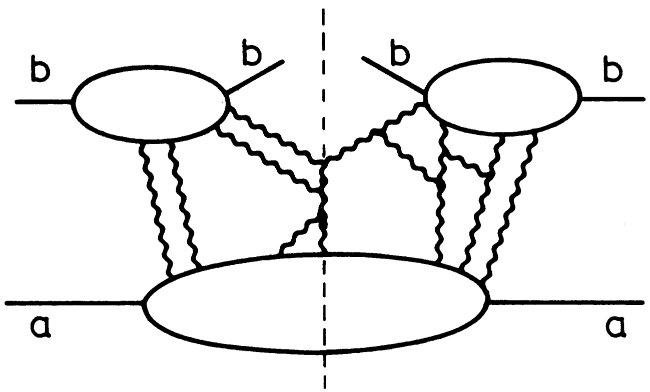

Fig. 1

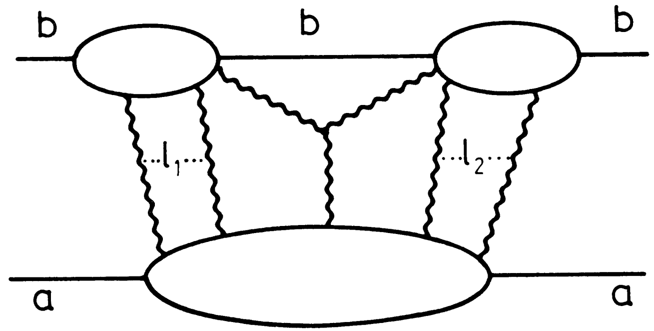

Fig. 2

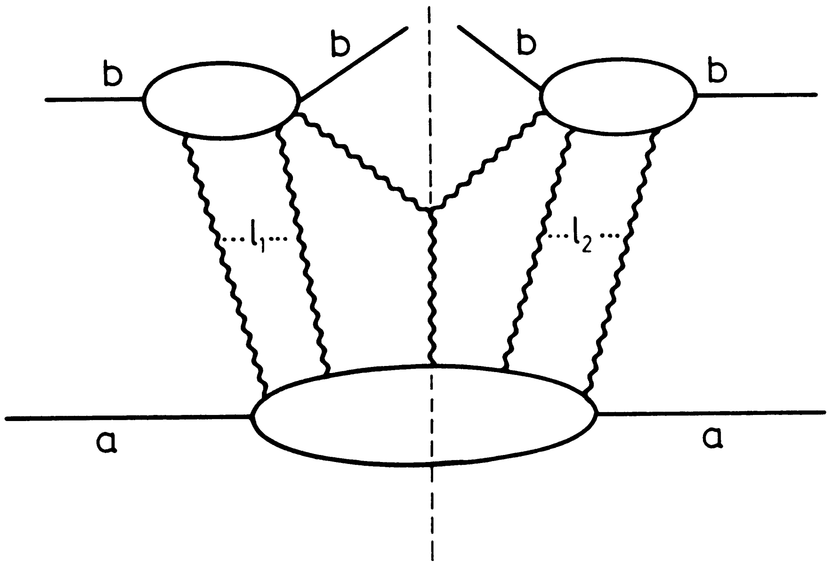

Fig. 3

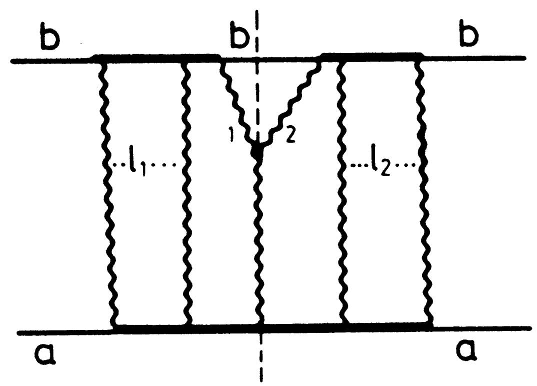

Fig. 4

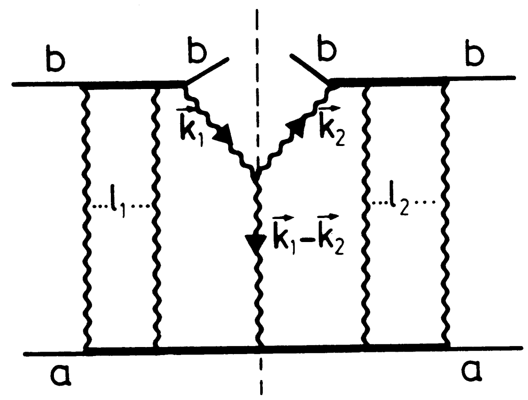

Fig. 5

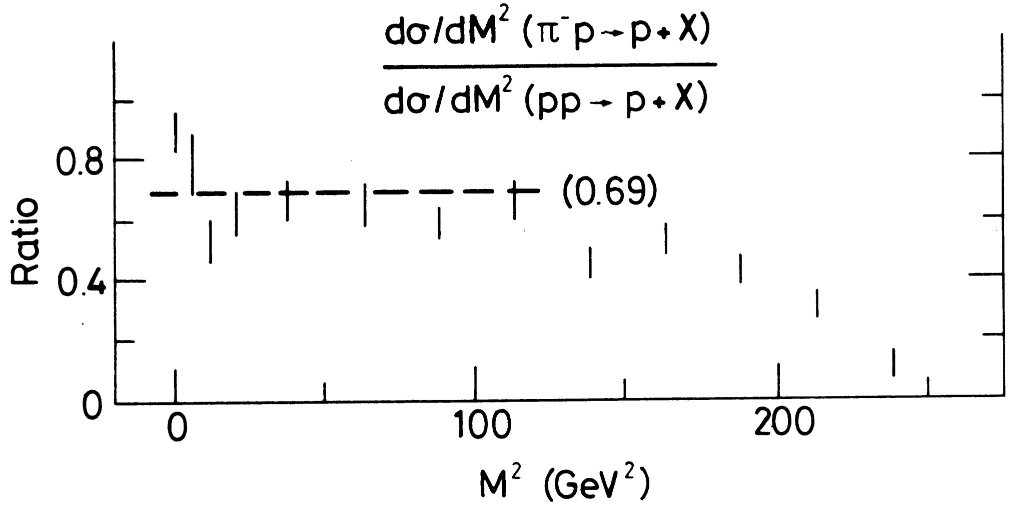

Fig. 6